Atmos. Chem. Phys. Discuss., 9, 25023–25047, 2009
www.atmos-chem-phys-discuss.net/9/25023/2009/


Atmospheric Chemistry and Physics Discussions

This discussion paper is/has been under review for the journal Atmospheric Chemistry and Physics (ACP). Please refer to the corresponding final paper in ACP if available.

# Chemical characterisation of iron in Dust and Biomass burning aerosols during AMMA-SOP0/DABEX: implication on iron solubility

**R. Paris**[1], **K. V. Desboeufs**[1], **P. Formenti**[1], **S. Nava**[2], **and C. Chou**[3]

[1]LISA, Universités Paris 12 et Paris 7, CNRS, Créteil, France
[2]National Institute of Nuclear Physics, Florence, Italy
[3]ETH, Institut für Atmosphäre und Klima, Zürich, Switzerland

Received: 12 October 2009 – Accepted: 12 November 2009 – Published: 25 November 2009

Correspondence to: R. Paris (rodolphe.paris@lisa.univ-paris12.fr)

Published by Copernicus Publications on behalf of the European Geosciences Union.





## Abstract

Chemical composition and the soluble fraction (in MilliQ water) has been determined in aerosol samples collected during flights of AMMA-SOP0/DABEX campaign conducted in the West African Sahel during dry season (2006). Two types of samples are encountered in this period: dust particles (DUST) and biomass burning aerosol (BB). Chemical analysis and microscope observations show that iron (Fe) found in BB samples is mainly issued from dust particles externally mixed in the biomass burning layer. Chemical analyses of samples show that solubilities determined for Fe in samples of African dust were significantly lower than the solubilities in aerosols of biomass burning. Our data provide a first idea of the variability of iron dust solubility in the source region (0.1% and 3.4%). We found a relationship between iron solubility/clay content/source which partly confirms that the variability of iron solubility in this source region is related to the character and origin of the aerosols themselves. In the biomass burning samples, no relationship could be found between Fe solubility and the concentrations of acid species ($SO_4^{2-}$,$NO_3^-$ or oxalate) nor the content of carbon (TC, OC, BC) so we are unable to determine what are the processes involved in this increase of iron solubility. In terms of the supply of soluble Fe to oceanic ecosystems on a global scale, the observed higher solubility for Fe in biomass burning could imply an indirect source of Fe to marine ecosystem, but these aerosols are probably not significant because the Sahara is easily the dominant source of Fe to the Atlantic.

## 1 Introduction

The North Atlantic Ocean is under the influence of mineral dust plumes transported from West Africa. Consequently, African dust is the major source of iron to this open ocean region (Sarthou et al., 2003). Its deposition may influence the rate of nitrogen fixation by microorganisms, and subsequently the global carbon cycle. Beside dust emission, the African continent is affected by strong biomass burning events all year



ACPD

9, 25023–25047, 2009



round due to widespread savannah fires, and agricultural fires. The event of biomass burning in Africa follows a well determined seasonal cycle related to the seasonal shift in the Inter-Tropical Convergence Zone (ITCZ). Thus, maximum emissions of anthropogenic biomass burning aerosol from the south regions of northern Africa occur during the dry season (December/January/February), with very few emissions occurring during August/September/November (Nwofor et al., 2007).

At the global scale, the major source of primary carbonaceous aerosols is biomass burning, due to forest fires and to the widespread use as fuel for heating homes and cooking (Ito and Penner, 2005). Recently, Luo et al. (2008) suggested that combustion iron (industry, biofuels and biomass burning) having a higher bioavailability, could represent 50% of the global iron deposition budget. However, the data on iron solubility from biomass burning are scarce; work of Luo et al. (2008) is essentially based on the measurements of Guieu et al. (2005) which emphasizes that biomass burning may be an important input of iron to the Mediterranean Sea relative to Saharan dust input. Because of the specific weather conditions and the greater diversity of vegetation types burned in forest fires, regional differences in biomass burning aerosol composition are expected. This implies that more work should be done to refine the assessment of the iron solubility of biomass burning sources. In this context, the international field campaign AMMA-DABEX (Analysis Multidisciplinary of African Monsoon – Dust and Biomass burning Experiment), conducted in Sahelian regions during the January-February dry season (2006) offered an excellent framework to study the solubility of iron from biomass burning and from mineral dust. Indeed, DABEX Special Observation Periods covered mainly the dry season over Niamey (Niger), which is a period dominated by minerals dust and biomass burning particles mixing events. In this paper, we present an estimation of the contribution of African dust and biomass burning aerosols, to the supply of iron soluble elements in the atmospheric deposition. To do so, we measured the water soluble fraction on aerosol samples collected onboard the aircraft FAAM Bae-146.



ACPD
9, 25023–25047, 2009



## 2 Material and method

### 2.1 Sampling

Instruments and samplers were operated onboard the UK Facility for Airborne Atmospheric Research (FAAM) BAe-146 research aircraft (http://www.faam.ac.uk/). The region of operation of the aircraft during the AMMA-SOP0/DABEX experiments and the full description of the aircraft and onboard instrumentation are presented in Haywood et al. (2008). The aerosol sampling system for filter collection consists of two stacked-filter units (SFUs) mounted in parallel. Samples were collected only during horizontal flight legs lasting not less than 20–30 min in order to guarantee sufficient loading of the filter samples. One SFU was used for measuring water-soluble ions and major, minor, and trace elements. In this case, SFU consisted of a Nuclepore filter of nominal pore size 0.4 $\mu$m, 90 mm. The second SFU was used for measuring carbonaceous aerosols. In this case, the sampling medium consisted of one Whatman QMA quartz filter, 47 mm. Quartz filters were pre-baked at 600°C for approximately 12 h to eliminate organic impurities. 57 filter samples had been collected during the 13 research flights of the BAe-146, performed from Niamey, Niger during AMMA-SOP0/DABEX. In parallel of aerosols sampling, we estimate the contamination of the method with the use of "blank filters". All details of sampling are described in Formenti et al. (2008). The identification and the details of operational sampling conditions of studied filters are summarized in Table 1.

### 2.2 Chemical composition

Total elemental concentrations for elements from Na to Pb (Note: TFe for Total elemental Fe), for all collected samples were measured by Particle-Induced X-ray Emission (PIXE) at the 3 MV Tandetron accelerator of the Labec laboratory (Formenti et al., 2008), with the external beam set-up described in Calzolai et al. (2006). PIXE spectra were fitted using the GUPIX code and elemental concentrations were obtained via a



ACPD
9, 25023–25047, 2009



calibration curve from a set of thin standards (Chiari et al., 2005); it should be noted that the concentrations of light elements, like Al, may be somewhat underestimated due to X-rays self-absorption inside aerosol particles (Marino et al., 2008). A two-step thermal method was applied for the separation and the analysis of black and organic carbon aerosol contents (BC and OC, respectively). The protocol (Cachier et al., 1989) consists firstly in an acidic step to remove carbonates; then, a thermal pre-treatment under pure $O_2$ and during 2 h was applied prior to the coulometric analysis (Ströhlein COULOMAT 702C) of carbon.

### 2.3 Water soluble fraction

Sample handling was performed in an ultra clean laboratory (class<1000) on ultra clean laminar flow benches (Class<10). Dissolution experiments to measure the water-soluble fraction of collected aerosols have been carried on 31 filters (over 57 collected): 13 DUST and 18 BB samples (13 BB1 and 5 BB2). To prepare the sample solution, one quarter of each SFU filters and blank filters was extracted using 100 mL water (of 18.2 MΩ $cm^{-1}$ resistance) by 30 min ultrasonic agitation. The solution was filtered on a 0.2 $\mu$m Nucleopore polycarbonate filter (Whatman). Inorganic and organic anions species ($Cl^-$, $Br^-$, $NO_2^-$, $NO_3^-$, $SO_3^{2-}$, $SO_4^{2-}$, acetate, formate, propionate, butyrate, MSA-, pyruvate, valerate, and oxalate) were quantified by ion chromatography. Ion chromatography (IC) analysis have been carried out with a Dionex 4500i device, equipped with an AS11-HC column associated with an AG11 pre-column. For simultaneous separation of inorganic and short-chain organic anions, gradient elution by 1–66 mM NaOH (1.5 mL/min) was employed. Dissolved iron concentration (DFe) was analysed by GFAAS (ATI-Unicam 929) (Sofikitis et al., 2004). Multi-elementary analysis of the dissolved phase was made by ICP-AES (PE Optima 3000) (Desboeufs et al., 2003).





## 3 Results and discussion

### 3.1 Characterisation of particulate iron

During AMMA-SOP0/DABEX campaign, mineral dust was generally observed at low altitudes (up to approximately 2 km) and a persistent layer of biomass burning aerosol was observed between 2 and 5 km, often in mixing with dust (Johnson et al., 2008). Based on visual observation and analysis of physical and optical measurements during flights, it was possible to distinguish the aerosol type of each layer (Formenti et al., 2008). Thus every samples collected in dust layers is noted "DUST" and biomass burning layers is noted "BB" (Table 1). Measurements of OC/OM (Organic Compounds and Organic Matter, respectively) in BB layers show no major anthropogenic fossil fuel pollution sources (Capes et al., 2008).

The total iron concentrations show lower values for samples collected in BB layers ($[Fe]_{tot}$= 7.8 ± 8.3 $\mu g.m^{-3}$) while DUST samples have concentrations almost twice as large ($[Fe]_{tot}$ = 15.9 ± 13.4 $\mu g\,m^{-3}$). The iron concentrations show a very good correlation with Al whatever the type of samples (Fig. 1). The ratio Fe/Al obtained during this study (Fe/Al=0.58) is in agreement with the values obtained at the ground-based site in Banizoumbou (Niger) during the same period (Fe/Al=0.56), mainly influenced by dust layer (Formenti et al., 2008; Rajot et al., 2008) and in general in the Saharan dust air masses (e.g. Kandler and Schutz, 2007; Lafon et al., 2006). Chemical analysis of individual particles by electronic microscope confirm the very low content of Fe in the biomass burning particles (mainly constituted by C, S and K) (Chou et al., 2008), indicating that even in BB layers, iron is due to mineral dust iron and not to combustion of vegetation. This is consistent with previous observations by Cachier et al. (1995) or Andreae et al. (1998) for African savannah fires. By approximation of the particulate mass on the filters from Al total content and the mass % of Al in the terrestrial crust (8.3%), the mass % of various elements has been estimated. The mass% of the elements typical of terrigeneous origin (Al, Fe, Si, Ti, Ca) in DUST and BB samples show



ACPD
9, 25023–25047, 2009



that the dust present in the BB samples are chemically similar to the dust in DUST samples.

Potassium is an important species emitted by biomass burning, and the fraction of potassium not related to sea-salt and soil dust could be used as a qualitative tracer for biomass combustion (Cachier and Ducret, 1991). Formenti et al. (2008) show correlation between K and Al, for BB samples, confirming the observation of mixing between dust and BB. The electronic microscope analysis seems to show that dust and biomass burning are externally mixed (Chou et al., 2008). In order to estimate, the contribution of mixing in the samples, the correlation K/Fe has been estimated for all DUST samples, a strong linear correlation is obtained and a ratio K/Fe in dust is estimated as 0.31 ($R^2 = 0.99$), from the slope of the regression curve. From this measurement, the *K* which originated from biomass burning has been estimated ($K_{exc}$) and plotted against the Fe concentration in BB (Fig. 2). Two kinds of correlation between $K_{exc}$ and Fe appear: (1) BB samples where a strong linear correlation is observed with $K_{exc}$/Fe=0.51 (noted group BB1), and (2) BB samples where $K_{exc}$ exhibits a little correlation with Fe and $K_{exc}$/Fe is around 0.17 (noted group BB2). Thus, it displays that the samples of the group BB2 are enriched in iron in comparison of group BB1. Assuming mixing between Dust and BB in all samples with $K_{exc}$, this means a more important contribution of dust in the samples of group BB2. To confirm this large contribution of dust in the group BB2, we estimated the total carbon (TC) on the filters via mass approximation with Al total content. We find that the average iron % in the two groups of BB and the DUST samples are close; 5.5% (±0.5%); 5.4% (±0.4%) and 5.1% (±0.3%), respectively. This corroborates that the iron is mainly issued from dust origin whatever the samples. For TC, the average % are 23.1% (±14.1%) for the group BB1 and 12.4% (±8.4%) for the group BB2, confirming a lower contribution of BB aerosols in this group. To explain the two types of correlation between Fe and K, we may suppose that these two groups are related to 2 types of mixing between dust and BB aerosols. It is known that the savannah fires induced an intense remobilisation of terrigenous particles deposed on the vegetation (Gaudichet et al., 1995). For the group BB1, as Fe and $K_{exc}$ are corre-



ACPD
9, 25023–25047, 2009



lated, the mixing happens probably directly in the biomass burning air masses due to the dust deposition on vegetation. The value of $K_{exc}$/Fe=0.51 for this group is comparable to the value found by Guieu et al. (2005) ($_{NSS}$K/Fe=0.63) in Mediterranean region close to source of summer forest fires. For the group BB2, the large part of iron concentrations could be due to the injection of new dust in the biomass burning air masses during their transport. Another explanation could be related to the evolution of the size distribution of aerosol in the BB air mass during its transport. The dust particles that are coarser than combustion particles could be removed by gravitational settling involving a decrease of Fe content in the air mass. However, the study of the size fraction in number, measured by PCASP (Osborne et al., 2008) contradict this assumption.

### 3.2 Water soluble fraction and iron solubility

The concentrations have been determined by IC and ICP-AES are shown in Table 2 (Note: 30% of iron measurement are not usable, mainly for BB filters, because the results are under the detection limit). The soluble fractions of typical elements of terrigeneous origin (Al, Fe, Si, Ti, and Ca) are similar in all the samples (BB and DUST). The results show that concentrations of dissolved K, P, $NO_3^-$, $SO_4^{2-}$ and $C_2O_4^{2-}$ are highest in the BB samples (at least by a factor 2), oxalate being even under limits of detection in all the DUST samples. The concentrations of dissolved P, $NO_3^-$, $SO_4^{2-}$ and $C_2O_4^{2-}$ present good correlation with those of dissolved K ($R^2$ between 0.6 and 0.9), as expected as they are derived from vegetation burning. The $SO_4^{2-}$/S ratio is 2.72, consistent with the value of 3 that would be obtained if the entire measured sulphur was present as water-soluble sulphate. It is known that near the emission, elementary K was mainly present as KCl, evolving to $K_2SO_4$ with aging of air masses (Gaudichet et al., 1995), due to secondary processing of $SO_2$ from biomass burning sources. Thus, the lower K/S is, the older the BB air masses are. Oxalate concentrations are anti-correlated with K/S ratio ($R^2 = 0.8$), thus indicating that biomass burning is the primary source of oxalate in the condensation mode.



ACPD
9, 25023–25047, 2009



The obtained iron soluble fraction (SFe) is detailed in the Fig. 3 as the ratio of dissolved to total iron (DFe/TFe). We found a median soluble fraction of 0.9%, 2.0%, and 2.2% respectively for the group DUST, BB2 and BB1.

### 3.2.1 Iron solubility in mineral Dust

It appears a large variability of the iron soluble fraction in DUST samples, solubility values range from 0.1% to 3.4%. These values are in good agreement with a number of other estimates for Fe solubility in Saharan dust in the zone of transport (e.g. Baker et al., 2006; Bonnet and Guieu, 2004; Johansen et al., 2000). For example, Baker et al. (2006) found Fe solubilities of Saharan dust with values extending from 1.4% to 4.1% over the Atlantic Ocean. To our knowledge, no data on the iron solubility exist so close to the dust source region in Africa, and our results represent the first measurement of the variability of solubility of Fe from mineral dust close to their African sources. To explain this variability, various works considered that the Fe solubility is a function of particle aerosol loading (Bonnet and Guieu, 2004; Baker et al., 2006). In our case, no relationship between iron solubility and dust concentration (estimated by Al content) was observed, indicating that particle concentration has a small effect on the dust Fe solubility. Moreover, from the measurement of particles size distribution by microscope observation of filters (Chou et al., 2008) and the study of number size fraction of different samples, no relationship appears between particle size and iron solubility. Recently, Journet et al. (2008) propose the essential role of mineralogical composition to estimate iron solubility. The Clays, and notably illite and montmorillonite, have a higher solubility of iron trapped in the crystal lattice of aluminosilicates. Due to the large abundance of clay minerals, it could provide more than 96% of DFe. Quantitative mineralogical composition of sampled dust is limited by the content of matter on the filter. Then it has been impossible to establish a relationship between the total iron content and SFe. In order to observe a potential effect of mineralogy, we compare the solubility of Mg, as a proxy of the dissolution of clay-containing Mg such as illite and montmorillonite, and that of Fe (Fig. 4, Diamonds). These results



ACPD
9, 25023–25047, 2009



emphasize a linear relationship between soluble fraction of iron and magnesium for several samples, suggesting that the dissolved iron could be issued from the dissolution of clay. Otherwise, the ratio SMg/SFe which is around 8, is in agreement with the ratio for pure illite or montmorillonite, extending from 3 to 8 (Journet et al., 2008). Thus, the variability of iron solubility could be related to the variability of clay content. Besides this correlation, samples (Fig. 4, circles) did not fit with the others. There are a couple of hypotheses to explain this very high SMg/SFe ratio measured with these aerosols samples. First of all, the important dissolution of Mg can be due to the contribution of other clays. For example, pure nontronite presents a ratio of 81 (Journet et al., 2008), a value comparable to the one in this study (around 50). Nevertheless, we cannot set aside the possibility of the presence of other non-Fe mineral containing Mg, which could lead to the increase of the soluble form of this element in the samples. To confirm the role of mineralogical composition of dust, we have carried out the study of back trajectories (http://www.ready.noaa.gov/ready/open/hysplit4.html) based on flight plan (Table 1). Calculating back trajectories from each vertical layer within the main dust plume enable to identify the source regions. This study shows that it seems to be a relationship between source regions and iron solubility. They are found to be very various from the Southern Algerian, Malian and Mauritanian deserts and also from Chad (Bodélé depression) or North Niger, in agreement with climatologically studies for this time of the year. The examination of the time series of SEVIRI dust observation indicates that active sources were the Bodélé region, with a peak in intensity on 21 January 2006 (B160N3), the 23 January 2006 (B161N5) and also on 30 January 2006 (B165N2). This influence is confirmed by the high content in Si in these samples and by the presence of diatoms by SEM (Scanning Electron Microscope) observations. These 3 "Bodélé samples" present the lowest iron solubility (around 0.15%). Thus, our results seem emphasize a relationship between iron solubility/clay content/source and hence partly confirm that the variability of iron solubility in this source region is related to the composition and origin of the aerosols themselves.



ACPD
9, 25023–25047, 2009



### 3.2.2 Iron solubility in biomass burning layers

The soluble iron for BB filters appears to be higher by 2 orders of magnitude than the DUST filters (Fig. 3). These observations are in agreement with the data of Guieu et al. (2005), who observed an increase of solubility of iron between dust and biomass burning air masses in Mediterranean region. Chuang et al. (2005) show the high solubility of Fe by anthropogenic emissions of combustion fuel by finding a correlation between BC and SFe. In the case of biomass burning air masses, no direct relationship exists between soluble Fe and the concentrations in BC, OC or TC, likewise for $K_{exc}$. Thus, biomass burning aerosols are not a significant direct source of soluble iron. Dust remains the major source of Fe even in the biomass burning air masses, and the mixing with combustion particles enables the increase of iron solubility. Besides, it appears that the observed variability on SFe in dust samples is also present for the BB samples, but shifted to higher values (Fig. 3). The presence of organic compounds as oxalate, or acid species as sulphate could explain the increase of Fe dust solubility in the BB samples, as observed by studies conducted over Atlantic Ocean or in Asian region (Chen and Siefert, 2004). However, these individual compounds exhibit only a little correlation with soluble Fe. It is probable that the large variability observed on iron solubility in dust explain this little correlation. The combustion process could also be a determining factor in the increase of solubility observed for the dust mixed with BB, for example by inducing chemical (reductive/oxidant) modifications of iron. It is effectively known that the oxidation state of iron at the surface of particles is highly dependent on the flame conditions (e.g. Jasinski et al., 2005). Desboeufs et al. (2005) show also that the solubility of iron from alumino-sicilated matrix is lowest in dust particles than in fly ash, which are issued from combustion process in power plant. The idea of the effect of combustion process on iron solubility is reinforced by the fact that the solubility of iron in the BB2, enriched in additional dust particles, is lowest than the solubility obtained in BB1 group. Finally, the results of this study emphasize that the iron in biomass burning air masses is dust-bearing iron and that its solubility is increased in comparison with



ACPD
9, 25023–25047, 2009



dust, which had not interacted with BB aerosols. The process explaining the increase of iron solubility from dust in biomass burning air masses is still not well known.

## 4 Conclusions

To conclude in terms of iron deposition, the mineral aerosols dominate above combustion sources by a factor above 30 at the global scale (Luo et al., 2008). As the dissolved concentrations measured in this study showed that iron is in the same order of magnitude ($DFe_{BB}$ =0.13 $\mu g\,m^{-3}$ vs. $DFe_{Dust}$ = 0.16 $\mu g\,m^{-3}$), the ratio of content of soluble iron between Dust and BB source should be around 30. Even if the biomass burning is not a direct source of soluble Fe, but due to the dust deposited on vegetation that are carried away, biomass burning could be a large indirect source of mineral Fe. However, the aerosols of biomass burning are probably not significant because the Sahara is easily the dominant source of Fe to the Atlantic. Among other elements, which present also a biogeochemical, interest is phosphorous. The element is known to be produced by biomass burning (e.g. Echalar et al., 1995). Due to the limit of detection of PIXE, we have little information on the content of particulate P. On the other hand, the data on dissolved P show that the BB samples releases more phosphorous (in average 0.15 $\mu g\,m^{-3}$) than the DUST samples (in average 0.08 $\mu g\,m^{-3}$) (Table 1). Based on our results, the BB air masses could constitute a large supplier of P to the Ocean, but also for S and N, whereas inputs of soluble Fe and Si are dominated by dust deposition.

*Acknowledgements.* Based on a French initiative, AMMA was built by an international scientific group and is currently funded by a large number of agencies, especially from France, the United Kingdom, the United States, and Africa. It has been the beneficiary of a major financial contribution from the European Community's Sixth Framework Research Programme. Detailed information on scientific coordination and funding is available on the AMMA International Web site at www.amma-international.org.

Financial support of the API-AMMA and the LEFE (project BIRD) national programs is acknowledged. The authors also wish to thank the BAe-146 air and ground crews, as well as the





FAAM and Met Office observers. H. Cachier and K. Oikonomou (LSCE, Gif sur Yvette, France) provided the analysis of total carbon.

The authors are also grateful to BAe-146 air and ground crews, as well as the FAAM and Met Office observers, and the AMMA-SOP0/DABEX PI J. Haywood (Met Office). They also thank the "Institut National des Sciences de l'Univers" (INSU/CNRS) for his support.


The publication of this article is financed by CNRS-INSU.

## References

Andreae, M. O., Andreae, T. W., Annegarn, H., Beer, J., Cachier, H., Le Canut, P., Elbert, W., Maenhaut, W., Salma, I., Wienhold, F. G., and Zenker, T.: Airborne studies of aerosol emissons from savanna fires in southern Africa, 2, aerosol chemical composition, J. Geophys. Res., 32, 119–128, 1998.

Baker, A. R., Jickells, T. D., Witt, M., and Linge, K. L.: Trends in the solubility of iron, aluminium, manganese and phosphorus in aerosol collected over the Atlantic Ocean, Mar. Chem., 98, 43–58, 2006.

Bonnet, S. and Guieu, C.: Dissolution of atmospheric iron in seawater, Geophys. Res. Lett., 31, L03303, doi:10.1029/2003GL018423, 2004.

Cachier, H.: Isotopic characterization of carbonaceous aerosols, Aerosol Sci. Tech., 10, 379–385, 1989.

Cachier, H. and Ducret, J.: Influence of biomass burning on equatorial african rains, Nature, 352, 228–230, 1991.

Cachier, H., Liousse, C., and Buat-Menard, P.: Particulate content of savanna fire emissions, J. Atmos. Chem., 22, 123–148, 1995.





Calzolai, G., Chiari, M., Garcia Orellana, I., Lucarelli, F., Migliori, A., Nava, S., and Taccetti, F.: The new external beam facility for environmental studies at the Tandetron accelerator of LABEC, Nucl. Instr. Meth., B249, 928–931, 2006.

Capes, G., Johnson, B., McFiggans, G., Williams, P. I., Haywood, J., and Coe, H.: Aging of biomass burning aerosols over west Africa: Aircraft measurements of chemical composition, microphysical properties, and emission ratios, J. Geophys. Res.-Atmos., 113, D00C15, doi:10.1029/2008JD009845, 2008.

Chen, Y. and Siefert, R. L.: Seasonal and spatial distributions and dry deposition fluxes of atmospheric total and labile iron over the tropical and subtropical North Atlantic Ocean, J. Geophys. Res., 109, D09305, doi:10.1029/2003JD003958, 2004.

Chiari, M., Lucarelli, F., Mazzei, F., Nava, S., Paperetti, L., Prati, P., Valli G., and Vecchi, R.: Characterization of airborne particulate matter in an industrial district near Florence by PIXE and PESA, Journal of X-Ray Spectrometry, 34(4), 323–329, 2005.

Chou, C., Formenti, P., Maille, M., Ausset, P., Helas, G., Harrison, M., and Osborne, S.: Size distribution, shape, and composition of mineral dust aerosols collected during the African Monsoon Multidisciplinary Analysis - Special Observation Period 0: Dust and Biomass-Burning EXperiment field campaign in Niger, January 2006, J. Geophys. Res.-Atmos., 113, D00C10, doi:10.1029/2008JD009897, 2008.

Chuang, P. Y., Duvall, R. M., Shafer, M. M., and Schauer, J. J.: The origin of water soluble particulate iron in the Asian atmospheric outflow, Geophys. Res. Lett., 32, L07813, doi:10.1029/2004GL021946, 2005.

Desboeufs, K. V., Losno, R., and Colin, J. L.: Figures of merit of pneumatic and ultrasonic sample introduction systems in Inductively Coupled Plasma-multichannel-based emission spectrometry in an ultra-clean environment, Anal. Bioanal. Chem., 375, 567–573, 2003.

Desboeufs, K. V., Sofikitis, A., Losno, R., Colin, J. L., and Ausset, P.: Dissolution and solubility of trace metals from natural and anthropogenic aerosol particulate matter, Chemosphere, 58, 195–203, 2005.

Echalar, F., Gaudichet, A., Cachier, H., and Artaxo, P.: Aerosol emissions by tropical forest and savanna biomass burning: Characteristic trace elements and fluxes, Geophys. Res. Lett., 22, 95GL03170, 3039–3042, 1995.

Formenti, P., Rajot, J. L., Desboeufs, K., Caquineau, S., Chevaillier, S., Nava, S., Gaudichet, A., Journet, E., Triquet, S., Alfaro, S., Chiari, M., Haywood, J., Coe, H., and Highwood, E.: Regional variability of the composition of mineral dust from western Africa: Results from





the AMMA-SOP0/DABEX and DODO field campaigns, J. Geophys. Res., 113, D00C13, doi:10.1029/2008JD009903, 2008.
Gaudichet, A., Echalar, F., Chatenet, B., Quisefit, J. P., Malingre, G., Cachier, H., Artaxo, P., Maenhaut, W., and Buat-Ménard, P.: Trace elements in tropical African savanna biomass burning aerosol, J. Atmos. Chem., 22, 19–39, 1995.
Guieu, C., Bonnet, S., Wagener, T., and Loye-Pilot, M. D.: Biomass burning as a source of dissolved iron to the open ocean?, Geophys. Res. Lett., 32, L19608, doi:10.1029/2005GL022962, 2005.
Haywood, J. M., Pelon, J., Formenti, P., Bharmal, N., Brooks, M., Capes, G., Chazette, P., Chou, C., Christopher, S., Coe, H., Cuesta, J., Derimian, Y., Desboeufs, K., Greed, G., Harrison, M., Heese, B., Highwood, E. J., Johnson, B., Mallet, M., Marticorena, B., Marsham, J., Milton, S., Myhre, G., Osborne, S. R., Parker, D. J., Rajot, J. L., Schulz, M., Slingo, A., Tanré, D., and Tulet, P.: Overview of the Dust And Biomass-burning EXperiment and African Monsoon Multidisciplinary Analysis Special Observing Period-0, J. Geophys. Res., 113, D00C17, doi:10.1029/2008JD010077, 2008.
Ito, A. and Penner, J. E.: Historical emissions of carbonaceous aerosols from biomass and fossil fuel burning for the period 1870–2000, Global Biogeochem. Cy., 19, GB2028, doi:10.1029/2004GB002474, 2005.
Jasinski, J., Pinkerton, K. E., Kennedy, I. M., and Leppert, V. J.: Surface oxidation state of combustion-synthesized [gamma]-$fe_2o_3$ nanoparticles determined by electron energy loss spectroscopy in the transmission electron microscope, Sensors and Actuators B: Chemical, 109, 19–23, 2005.
Johansen, A. M., Siefert, R. L., and Hoffmann, M. R.: Chemical composition of aerosols collected over the tropical north atlantic ocean, J. Geophys. Res., 105, 15277–15312, 2000.
Johnson, B. T., Osborne, S. R., Haywood, J. M., and Harrison, M. A. J.: Aircraft measurements of Biomass Burning Aerosol Over west Africa during DABEX, J. Geophys. Res.-Atmos., 113, D00C06, doi:10.1029/2007JD009451, 2008.
Journet , E., Desboeufs, K. V., Caquineau, S., and Colin, J. L.: Mineralogy as a critical factor of dust iron solubility, Geophys. Res. Lett., 35, L07805, doi:10.1029/2007GL031589, 2008.
Kandler, K. and Schutz, L.: Climatology of the average water-soluble volume fraction of atmospheric aerosol, Atmos. Res., 83, 77–92, 2007.
Lafon, S., Sokolik, I. N., Rajot, J. L., Caquineau, S., and Gaudichet, A.: Characterization of iron oxides in mineral dust aerosols: Implications for light absorption, J. Geophys. Res., 111,





D21207, doi:10.1029/2005JD007016, 2006.
Luo, C., Mahowald, N., Bond, T., Chuang, P. Y., Artaxo, P., Siefert, R., Chen, Y., and Schauer, J.: Combustion iron distribution and deposition, Global Biogeochem. Cy., 22, GB1012, doi:10.1029/2007GB002964, 2008.
Marino, F., Calzolai, G., Caporali, S., Castellano, E., Chiari, M, Lucarelli, F., Maggi, V., Nava, S., Sala, M., and Udisti, R.: PIXE and PIGE techniques for the analysis of Antarctic ice dust and continental sediments, Nucl. Instrm. Meth. B, 266, 2396–2400, 2008.
Nwofor, O. K., Chineke, T. C., and Pinker, R. T.: Seasonal characteristics of spectral aerosol optical properties at a sub-saharan site, Atmos. Res., 85, 38–51, 2007.
Osborne, S. R., Johnson, B. T., Haywood, J. M., Baran, A. J., Harrison, M. A. J., and McConnell, C. L.: Physical and optical properties of mineral dust aerosol during the Dust and Biomass-burning Experiment, J. Geophys. Res., 113, D00C03, doi:10.1029/2007JD009551, 2008.
Rajot, J. L., Formenti, P., Alfaro, S., Desboeufs, K., Chevaillier, S., Chatenet, B., Gaudichet, A., Journet, E., Marticorena, B., Triquet, S., Maman, A., Mouget, N., and Zakou, A.: AMMA dust experiment: An overview of measurements performed during the dry season special observation period (sop0) at the banizoumbou (niger) supersite, J. Geophys. Res.-Atmos., 113, D00C14, doi:10.1029/2008JD009906, 2008.
Sarthou, G., Baker, A. R., Blain, S., Achterberg, E. P., Boye, M., Bowie, A. R., Croot, P., Laan, P., de Baar, H. J. W., Jickells, T. D., and Worsfold, P. J.: Atmospheric iron deposition and sea-surface dissolved iron concentrations in the eastern Atlantic ocean, Deep Sea Res. I, 50, 1339–1352, 2003.
Sofikitis, A. M., Colin, J.-L., Desboeufs, K. V., and Losno, R.: Iron analysis in atmospheric water samples by Atomic Absorption Spectroscopy (AAS) in water-methanol, Anal. Bioanal. Chem., 378, 460–464, 2004.





**Table 1.** Sample Identification and Main Operational Details for the Sampled Filter.

| DATE | SAMPLE ID | LOCATION | Lat (°,dec°) | Lon (°,dec°) | Altitude (km) |
|---|---|---|---|---|---|
| 16 JAN 2006 | B157N1 | Niger/Nigeria | 12.6 | 3.9 | 2.4 |
| | | | 11.3 | 4.3 | |
| 16 JAN 2006 | B157N2 | Niger/Nigeria | 11.1 | 4.3 | 2.0 |
| | | | 9.9 | 4.3 | |
| 16 JAN 2006 | B157N3 | Niger/Nigeria | 10.4 | 4.3 | 1.2–0.7 |
| | | | 11.5 | 4.1 | |
| 16 JAN 2006 | B157N4 | Niger/Nigeria | 11.7 | 2.4 | 0.5 |
| | | | 13.5 | 3.2 | |
| 16 JAN 2006 | B157N5 | Niger/Nigeria | 13.5 | 2.4 | 2.7 |
| | | | 13.6 | 3.2 | |
| 17 JAN 2006 | B158N1 | Niger/Nigeria | 12.3 | 3.8 | 3.3 |
| | | | 12.1 | 4.2 | |
| 17 JAN 2006 | B158N2 | Niger/Nigeria | 11.8 | 4.3 | 1.7–2.1 |
| | | | 10.3 | 4.3 | |
| 17 JAN 2006 | B158N3 | Niger/Nigeria | 9.8 | 4.3 | 0.8–1.6 |
| | | | 8.4 | 4.3 | |
| 17 JAN 2006 | B158N4 | Niger/Nigeria | 8.3 | 4.3 | 2–3 |
| | | | 8.3 | 4.3 | |
| 17 JAN 2006 | B158N5 | Niger/Nigeria | 11.0 | 4.3 | 0.6 |
| | | | 12.0 | 4.3 | |
| 17 JAN 2006 | B158N6 | Niger/Nigeria | 12.2 | 4.1 | 1.6–2 |
| | | | 12.6 | 3.6 | |



ACPD
9, 25023–25047, 2009



**Table 1.** Continued.

| DATE | SAMPLE ID | LOCATION | Lat (°,dec°) | Lon (°,dec°) | Altitude (km) |
|---|---|---|---|---|---|
| 19 JAN 2006 | B159N1 | Niger/Benin | 13.6 | 2.5 | 3.3 |
| | | | 13.4 | 1.9 | |
| 19 JAN 2006 | B159N2 | Niger/Benin | 13.4 | 1.8 | 2.7 |
| | | | 13.5 | 2.6 | |
| 19 JAN 2006 | B159N3 | Niger/Benin | 13.6 | 2.7 | 1.7 |
| | | | 13.4 | 1.9 | |
| 19 JAN 2006 | B159N4 | Niger/Benin | 13.4 | 2.1 | 0.15 |
| | | | 13.6 | 13.6 | |
| 19 JAN 2006 | B159N5 | Niger/Benin | 12.9 | 2.5 | profile |
| | | | 11.2 | 2.6 | |
| 19 JAN 2006 | B159N6 | Niger/Benin | 11.0 | 2.6 | 0.15 |
| | | | 9. 8 | 1.6 | |
| 19 JAN 2006 | B159N7 | Niger/Benin | 9.8 | 1.6 | 1.7–2.3 |
| | | | 12.2 | 2.4 | |
| 19 JAN 2006 | B159N8 | Niger/Benin | 12.4 | 2.3 | 2.0 |
| | | | 13.2 | 2.1 | |
| 21 JAN 2006 | B160N1 | North Niger | 13.7 | 2.6 | 3–3.3 |
| | | | 15.0 | 4.3 | |
| 21 JAN 2006 | B160N2 | North Niger | 15.1 | 4.4 | 2.5 |
| | | | 15.9 | 4.9 | |
| 21 JAN 2006 | B160N3 | North Niger | 16.1 | 4.9 | 1.7–1.0 |
| | | | 18.5 | 6.9 | |
| 21 JAN 2006 | B160N4 | North Niger | 18.4 | 6.9 | 1.2 |
| | | | 18.2 | 5.9 | |
| 21 JAN 2006 | B160N6 | North Niger | 14.6 | 3.6 | 2.7 |
| | | | 14.0 | 2.8 | |



ACPD

9, 25023–25047, 2009



**Table 1.** Continued.

| DATE | SAMPLE ID | LOCATION | Lat (°,dec°) | Lon (°,dec°) | Altitude (km) |
|---|---|---|---|---|---|
| 23 JAN 2006 | B161N1 | North Niger | 14.2<br>15.1 | 3.2<br>4.5 | 4.0 |
| 23 JAN 2006 | B161N2 | North Niger | 15.2<br>16.1 | 4.6<br>5.8 | 3.3 |
| 23 JAN 2006 | B161N3 | North Niger | 16.4<br>17.2 | 6.1<br>7.1 | 1.0 |
| 23 JAN 2006 | B161N5 | North Niger | 17.3<br>16.7 | 7.4<br>6.6 | 1.0 |
| 23 JAN 2006 | B161N6 | North Niger | 16.3<br>13.9 | 6.0<br>2.9 | 0.15–1.0 |
| 24 JAN 2006 | B162N1 | Niger/Nigeria | 12.3<br>10.6 | 2.4<br>2.9 | 3.7 |
| 24 JAN 2006 | B162N2 | Niger/Nigeria | 10.4<br>9.8 | 3.1<br>3.5 | 3.7 |
| 24 JAN 2006 | B162N3 | Niger/Nigeria | 11.2<br>11.2 | 4.0<br>3.5 | 0.7 |
| 24 JAN 2006 | B162N4 | Niger/Nigeria | 11.1<br>11.2 | 3.5<br>3.5 | 0.7–0.9 |
| 26 JAN 2006 | B163N1 | Around Niamey | 13.5<br>13.6 | 2.3<br>2.7 | 2.3-3.8 |
| 26 JAN 2006 | B163N2 | Around Niamey | 13.7<br>13.3 | 2.8<br>1.8 | 0.6–1.2 |
| 26 JAN 2006 | B163N4 | Around Niamey | 13.6<br>13.4 | 2.7<br>1.9 | 2.1-3.5 |
| 26 JAN 2006 | B163N5 | Around Niamey | 13.6<br>13.4 | 2.9<br>1.9 | 0.15 |



ACPD
9, 25023–25047, 2009



**Table 1.** Continued.

| DATE | SAMPLE ID | LOCATION | Lat (°,dec°) | Lon (°,dec°) | Altitude (km) |
|---|---|---|---|---|---|
| 29 JAN 2006 | B164N1 | Around Niamey | 13.6 | 2.3 | 3.5 |
| | | | 13.5 | 2.2 | |
| 29 JAN 2006 | B164N3 | Around Niamey | 13.5 | 2.3 | 1.2 |
| | | | 13.5 | 2.2 | |
| 29 JAN 2006 | B164N4 | Around Niamey | 13.5 | 2.3 | 0.6 |
| | | | 13.5 | 2.2 | |
| 30 JAN 2006 | B165N1 | North Niger | 13.9 | 3.2 | 3.3 |
| | | | 14.6 | 3.9 | |
| 30 JAN 2006 | B165N2 | North Niger | 14.9 | 4.3 | 1.0–1.2 |
| | | | 17.4 | 7.4 | |
| 30 JAN 2006 | B165N3 | North Niger | 16.4 | 5.9 | 1.9 |
| | | | 15.3 | 4.7 | |
| 30 JAN 2006 | B165N4 | North Niger | 14.6 | 4.0 | 3.8 |
| | | | 13.7 | 2.9 | |
| 30 JAN 2006 | B165N7 | North Niger | 13.6 | 2.8 | 0.15 |
| | | | 13.4 | 2.8 | |
| 1 FEB 2006 | B166N1 | Niger/Nigeria | 12.1 | 3.4 | 3.3 |
| | | | 10.5 | 5.1 | |
| 1 FEB 2006 | B166N2 | Niger/Nigeria | 10.3 | 5.3 | 1.5 |
| | | | 9.7 | 6.0 | |
| 1 FEB 2006 | B166N3 | Niger/Nigeria | 9.7 | 5.9 | 1.0 |
| | | | 9.7 | 5.0 | |
| 1 FEB 2006 | B166N4 | Niger/Nigeria | 10.1 | 5.0 | 0.8 |
| | | | 10.1 | 5.0 | |
| 1 FEB 2006 | B166N5 | Niger/Nigeria | 9.8 | 5.0 | 0.36–0.42 |
| | | | 9.9 | 6.0 | |
| 1 FEB 2006 | B166N6 | Niger/Nigeria | 9.9 | 5.8 | 0.4–0.45 |
| | | | 9.9 | 5.0 | |
| 1 FEB 2006 | B166N7 | Niger/Nigeria | 9.9 | 5.1 | 0.42 |
| | | | 9.9 | 6.0 | |
| 1 FEB 2006 | B166N8 | Niger/Nigeria | 10.6 | 5.0 | 2.7 |
| | | | 11.5 | 3.9 | |



ACPD
9, 25023–25047, 2009



**Table 2.** Concentrations of dissolved species ($\mu g\,m^{-3}$) in the water-soluble fraction of BB and DUST samples (DL: Detection Limit).

| | BB | | | DUST | | |
|---|---|---|---|---|---|---|
| | average | min | max | average | min | max |
| Al | 0.21 | 0.05 | 0.48 | 0.31 | 0.01 | 0.95 |
| Ca | 4.49 | 1.71 | 12.52 | 5.91 | 0.45 | 16.79 |
| Fe | 0.13 | 0.01 | 0.43 | 0.16 | 0.01 | 0.55 |
| K | 2.16 | 0.77 | 4.28 | 0.88 | 0.03 | 3.2 |
| P | 0.15 | 0.10 | 0.18 | 0.08 | 0.01 | 0.12 |
| $SO_4^{2-}$ | 3.86 | 2.14 | 5.41 | 2.32 | 1.38 | 4.09 |
| $NO_3^-$ | 5.08 | 2.53 | 7.42 | 1.78 | 0.58 | 4.54 |
| $C_2O_4^{2-}$ | 0.99 | 0.50 | 1.44 | <DL | | |



ACPD
9, 25023–25047, 2009



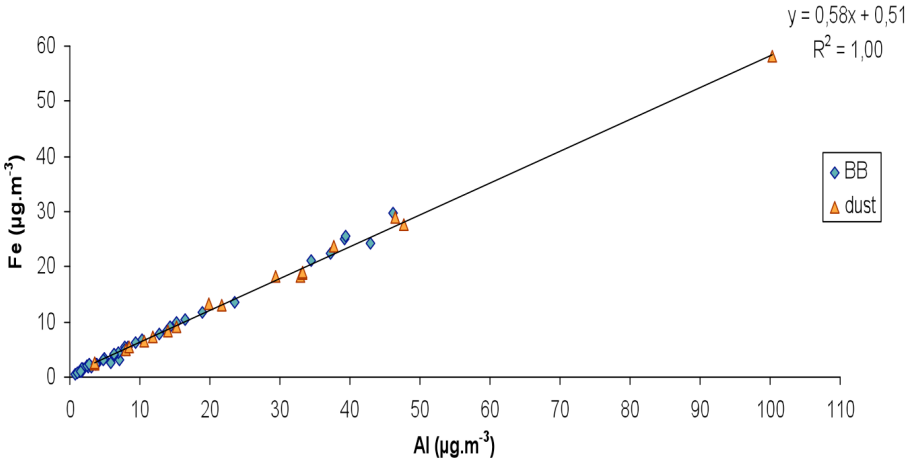


**Fig. 1.** Total Fe vs. Total Al for the entire DUST and BB aerosol samples.



ACPD
9, 25023–25047, 2009



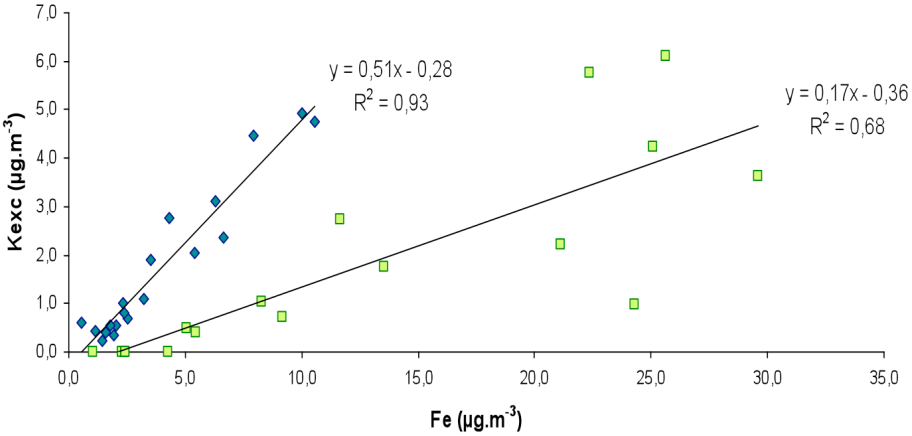


**Fig. 2.** Plot of Total Fe vs. Kexc in BB samples: two linear relations identified as BB1 group (diamond) and BB2 group (square) are observed.



ACPD
9, 25023–25047, 2009



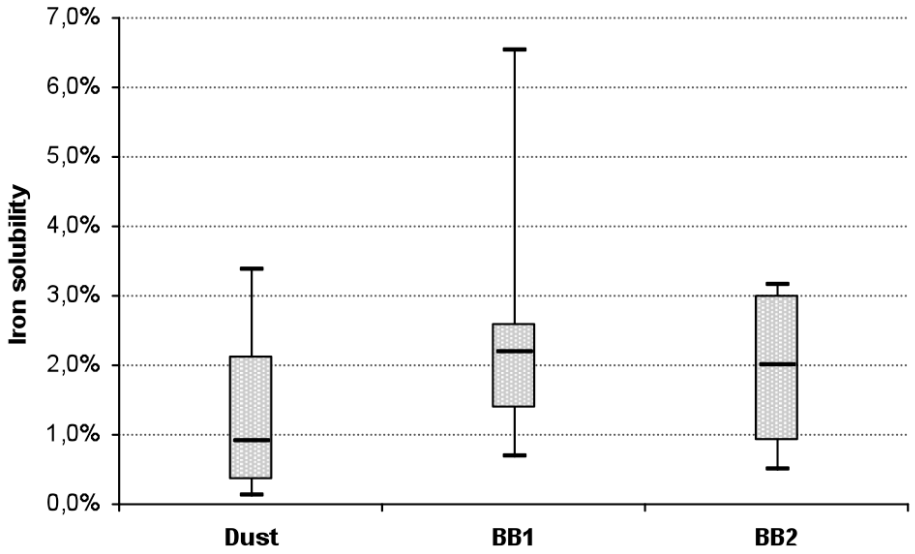


**Fig. 3.** Boxplot of Percentage solubility estimates of Fe for the 3 kinds of identified samples: dust, BB1 and BB2. Whiskers are from minimum to maximum, box width represents the interquartile range and a stroke is plotted inside of the box to represent the median.



ACPD
9, 25023–25047, 2009



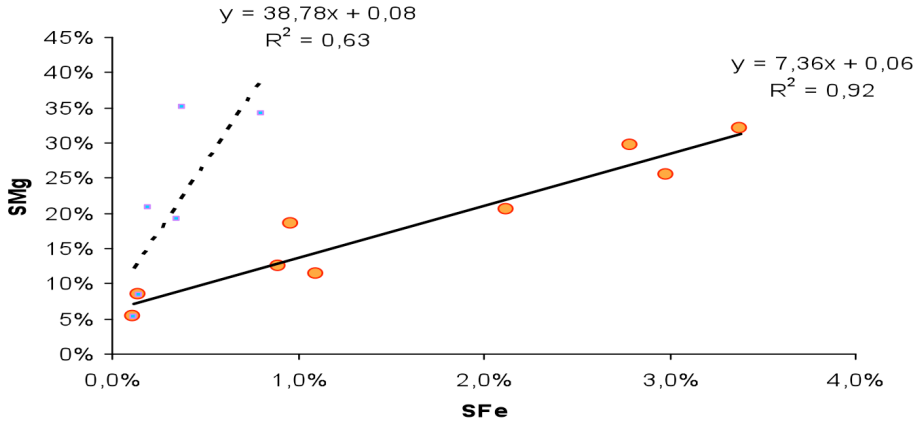


**Fig. 4.** Plot of percentage of SFe vs. SMg for all DUST samples. The two sets of points highlight the difference of mineralogy in the dust samples, characterized by different ratio.



ACPD
9, 25023–25047, 2009